Transition probabilities for piecewise affine models of genetic networks

Madalena Chaves, Etienne Farcot, Jean-Luc Gouzé

▶ **To cite this version:**

Madalena Chaves, Etienne Farcot, Jean-Luc Gouzé. Transition probabilities for piecewise affine models of genetic networks. Proc. Int. Symp. Mathematical Theory of Networks and Systems (MTNS 10), Budapest, Hungary, Jul. 2010., 2010, Budapest, Hungary. hal-00831793

HAL Id: hal-00831793
https://inria.hal.science/hal-00831793

Submitted on 7 Jun 2013

HAL is a multi-disciplinary open access archive for the deposit and dissemination of scientific research documents, whether they are published or not. The documents may come from teaching and research institutions in France or abroad, or from public or private research centers.

L'archive ouverte pluridisciplinaire **HAL**, est destinée au dépôt et à la diffusion de documents scientifiques de niveau recherche, publiés ou non, émanant des établissements d'enseignement et de recherche français ou étrangers, des laboratoires publics ou privés.

Transition probabilities for piecewise affine models of genetic networks

Madalena Chaves, Etienne Farcot and Jean-Luc Gouzé

***Abstract*— In the piecewise affine framework, trajectories evolve among hyperrectangles in the state space. A qualitative description of the dynamics - useful for models of genetic networks - can be obtained by viewing each hyperrectangle as a node in a discrete system, so that trajectories follow a path in a transition graph. In this paper, a probabilistic interpretation is given for the transition between two nodes A and B, based on the volume of the initial conditions on hyperrectangle A whose trajectories cross to B. In an example consisting of two intertwinned negative loops, this probabilistic interpretation is used to predict the most likely periodic orbit given a set of parameters, or to find parameters such that the system yields a desired periodic orbit with a high probability.**

I. INTRODUCTION

The class of piecewise affine (PWA) systems is a commonly used formalism to describe biological regulatory networks [5]. It provides a qualitative description of the dynamical behaviour, roughly by dividing the (continuous) state space into finitely many hyperrectangles, also called *domains*, and then describing the possible transitions between those domains [8], [1]. The state space of PWA networks can be described by a discrete system, where each discrete state represents a domain, and the transition graph between the states represents the pathways allowed for the trajectories of the continuous system. In general, there may be multiple transitions from the same domain, and in this case the transition graph provides no information on which transition is "more likely".

In this study, we explore the idea of associating a *probability* of transition to each of the edges in the discrete transition graph, in terms of the parameters of the PWA model (Section III; see also [7], for a first approach). If the transition probabilities between domains can be experimentally measured, this idea could be applied to estimate some of the model's parameters.

This method is also of interest in the case of a system whose asymptotic behaviour consists of a transition graph with no single state attractor, but with several transition cycles, raising the question of the existence of periodic trajectories [2] (Section IV). Some problems to be discussed include finding sets of parameters that lead to a given periodic trajectory, and to control the system from one periodic trajectory to another, by appropriately changing the inputs/parameters (Section V).

This work was supported in part by the INRIA-INSERM project ColAge.

M. Chaves and J.-L. Gouzé are with COMORE, INRIA, 2004 Route des Lucioles, BP 93, 06902 Sophia Antipolis, France. E. Farcot is with Virtual Plants, INRIA, Avenue Agropolis, 34398 Montpellier, France.

{mchaves,efarcot,gouze}@sophia.inria.fr

II. PIECEWISE AFFINE DIFFERENTIAL MODELS

Piecewise affine (PWA) differential systems where first introduced by Glass and co-authors [5] as suitable models for genetic regulatory models. Various mathematical aspects of these systems have recently been studied in detail [8], [1], including the definition of solutions across thresholds, sliding mode solutions, and the stability of steady states. The existence of periodic orbits for these systems has been studied, for instance in [6], [2], [4], as well as some control problems [3].

A. The general set up

Consider an n-dimensional system, $x \in \mathbb{R}^n$,

$$\dot{x} = f(x) - \Gamma x \tag{1}$$

where $f(x)$ is a piecewise constant function and $\Gamma = \text{diag}(\gamma_1, \ldots, \gamma_n)$. The function f represents the interactions between the various components of the system, for instance, the activation or inhibition effects between different proteins (see the example in Section IV). A general hypothesis underlying this class of models is the idea that a protein A_1 will strongly influence another protein A_2 once it reaches an appropriate concentration $\theta_{1\to 2}$; below this threshold concentration, A_1 does not influence A_2. To characterize the function f, we will assume that each variable i has r_i *thresholds*:

$$0 < \theta_i^1 < \cdots < \theta_i^{r_i} < M_i := \theta_i^{r_i+1}, \tag{2}$$

where $M_i = \max\{\frac{f_i(x)}{\gamma_i} : \ x \in \mathbb{R}_{\geq 0}\}$. These thresholds partition the state space into *regular domains* in which the vector fields are given by a linear function. To label these domains, we will use the notation:

$$B^{k_1\, k_2 \cdots k_n} : \quad k_i \in \{0, 1, \ldots, r_i\}, \quad \theta_i^{k_i} < x_i < \theta_i^{k_i+1},$$

with $\theta_i^0 := 0$. So, for $n = 3$ and $(r_1, r_2, r_3) = (1, 2, 2)$, B^{102} denotes the cube $x \in (\theta_x^1, M_x)$, $y \in (0, \theta_y^1)$, and $z \in (\theta_z^2, M_z)$. The segments defining the borders of the regular domains are called *switching domains*, since a group I_s (nonempty) of the variables is at a threshold value, and are denoted by:

$$D^{l_1 \cdots l_n} : \ \ l_i = \theta_i^{k_i}, i \in I_s, \ \ l_j = k_j, j \notin I_s.$$

In this paper, the function f takes a constant value in each regular domain: $f(x) = f^{k_1\, k_2 \cdots k_n}$, so that an expression for the solution of the system $\dot{x} = f^{k_1\, k_2 \cdots k_n} - \Gamma x$ can be explicitly written for each regular domain. The point $\phi^{k_1\, k_2 \cdots k_n} = (f_i^{k_1\, k_2 \cdots k_n}/\gamma_1, \ldots, f_n^{k_1\, k_2 \cdots k_n}/\gamma_n)$ is called the *focal point* of the domain $B^{k_1\, k_2 \cdots k_n}$. If $\phi^{k_1\, k_2 \cdots k_n} \in B^{k_1\, k_2 \cdots k_n}$, then

the focal point is an equilibrium of the system. The solutions of the system are thus continuous functions, and can be formed by concatenating the segments from each domain. The crossing between two regular domains (the function f is not defined at switching domains) can be defined in a natural way if the vector fields are not opposing on each side of the boundary [1]. Otherwise, solutions can still be defined, in the sense of Filippov [8].

B. Transition graph

For a trajectory starting in a given domain $B^{k_1 \cdots k_n}$ there are two possibilities: (i) if the domain contains its focal point $\phi^{k_1\, k_2 \cdots k_n}$, then this is actually an asymptotically stable equilibrium point and the trajectory will remain in $B^{k_1 \cdots k_n}$ for all times; (ii) if the focal point $\phi^{k_1\, k_2 \cdots k_n} \notin B^{k_1 \cdots k_n}$, then the trajectory will leave $B^{k_1 \cdots k_n}$ at some instant. In case (ii), the trajectory will leave the domain $B^{k_1 \cdots k_n}$ as soon as one of the variables reaches a threshold. Suppose that variable k_l is the first to reach a threshold; then we say that there is a transition

$$B^{k_1 \cdots k_n} \;\rightarrow\; B^{k_1 \cdots \tilde{k}_l \cdots k_n}, \quad \tilde{k}_l \in \{k_l - 1, k_l + 1\}.$$

The family of all possible one-variable transitions among the regular domains is called the *transition graph* of system (1) (see Fig. 3 for an example). In this graph, any domain B may have at most n *successors* $\mathcal{S}(B) \subset \{B^{\tilde{k}_1 \cdots k_n}, \ldots, B^{k_1 \cdots \tilde{k}_n}\}$.

Note that there are also trajectories for which two or more variables simultaneously reach their respective threshold values. These trajectories give rise to *separatrix* curves, since they partition the domain $B^{k_1 \cdots k_n}$ into regions that switch to the different possible successors in $\mathcal{S}(B)$ (see more details in Section III). However, the family of all separatrix curves forms a subset of measure zero of the set of all possible trajectories of system (1). Thus, for the results in this paper, one can assume that the one-variable switch *transition graph* does represent all the possible pathways for a trajectory of system (1).

One can also define the following object (see also [2]).

Definition 2.1: A sequence of L regular domains

$$B^{r_1} \rightarrow \cdots \rightarrow B^{r_L} \rightarrow B^{r_1}$$

that can be visited in one-variable transitions returning to the first domain after L transitions is called a *transition cycle of length L*.

Note that any periodic solution of (1) will follow a transition cycle, but the existence of a transition cycle does not imply the existence of a periodic orbit.

In this paper, we will assume that there are at most two successors for each region:

H1 Given any $B^r = B^{k_1\, k_2 \cdots k_n}$, there exist at most two coordinates x_i, x_j such that

$$\mathcal{S}(B^r) = \{\, B^i,\, B^j \,\},$$

where $B^i = B^{k_1 \cdots \tilde{k}_i \cdots k_n}$, $B^j = B^{k_1 \cdots \tilde{k}_j \cdots k_n}$ and $\tilde{k}_i \in \{k_i - 1, k_i + 1\}$ and $\tilde{k}_j \in \{k_j - 1, k_j + 1\}$.

In this case, a trajectory starting from any initial condition in B^r will either cross to B^i or B^j, dividing B^r into two subregions.

III. TRANSITION PROBABILIIES IN THE GRAPH

The transition graph contains information on the possible pathways for a trajectory, but it provides no indication on whether a given pathway is more likely than another. The goal of the present analysis is to relate dynamical aspects determined by the systems's parameters (here, synthesis and degradation rates) to *probabilities* of transition between two state space regions.

Under hypothesis H1, the transition from B^r to B^i or B^j can be studied in the 2D plane (x_i, x_j). For convenience of notation, let $x = x_i$, $y = x_j$ and $B^x = B^i$, $B^y = B^j$. To analyse the dynamics in B^r, it is enough to look at the projection of the space onto the plane x-y:

$$\dot{x} \;=\; f_x^r - \gamma_x x \tag{3}$$

$$\dot{y} \;=\; f_y^r - \gamma_y y, \tag{4}$$

where $f_x^r, f_y^r \geq 0$. Assume that θ_x^r and θ_y^r are the thresholds that will be crossed, and consider also the two closest thresholds for each variable: $\theta_x^{r-1} < \theta_x^r < \theta_x^{r+1}$, $\theta_y^{r-1} < \theta_y^r < \theta_y^{r+1}$. Then, the locus of the initial points from which a trajectory ends in (θ_x^r, θ_y^r) is a separatrix curve dividing the region B^r into two subsets from which transitions are possible to B^x or B^y. This curve can be easily computed from the solutions on B^r:

$$\begin{aligned} x(t) &= (x_0 - M_x)\exp^{-\gamma_x t} + M_x \\ y(t) &= (y_0 - M_y)\exp^{-\gamma_y t} + M_y \end{aligned}$$

letting $M_x = \frac{f_x^r}{\gamma_x}$ (similarly for M_y). The separatrix is:

$$\sigma(x) = y = M_y + (\theta_y^r - M_y)\left(\frac{x - M_x}{\theta_x^r - M_x}\right)^{\frac{\gamma_y}{\gamma_x}}. \tag{5}$$

To relate kinetic parameters to probabilities of transition, one idea is to compare the *volumes* of the two subregions of B^r above and below the separatrix [7]: that is, the probability of crossing from B^r to B^x would be given by the fraction of the volume of B^r corresponding to initial conditions that evolve to B^x. This has a natural biological interpretation as follows. Suppose a given experiment is repeated N times, always with initial conditions in B^r (that is, initial concentrations in the intervals defined by B^r) and one counts the number of times N_x that the system evolves to B^x. Then the quotient N_x/N can be viewed as the probability that trajectories of system (3) switch from B^r to B^x.

However, a careful look at Fig. 1 shows that more accurate probabilities should take into account the history of the trajectory. Indeed, on the upper panel of Fig. 1, if the trajectory enters the box B^r from the region $x < \theta_x^{r-1}$, $\theta_y^r < y < \theta_y^{r+1}$, then it will always proceed to B^x, by uniqueness of solutions inside B^r. In the next subsections, we explicitly calculate the area below the separatrix as a function of the systems parameters, and then suggest a definition for probability of transition that uses both the current box and the previous box.

A. Volume of initial conditions below the separatrix

For a general domain B^r, let (θ_x^r, θ_y^r) denote the ending point of the separatrix, and define

$$H(x) = \begin{cases} 1, & x > \theta_x^r \\ -1, & x < \theta_x^r \end{cases}$$

Then, one can see that $(x, y) \in B^r$ iff

$$\min\{\theta_x^r, \theta_x^{r+H(x)}\} < x < \max\{\theta_x^r, \theta_x^{r+H(x)}\},$$
$$\min\{\theta_y^r, \theta_y^{r+H(y)}\} < y < \max\{\theta_y^r, \theta_y^{r+H(y)}\}.$$

There are two possibilities for the starting point of the separatrix depending on whether the curve hits a vertical or horizontal threshold first (see the top and bottom plots in Fig. 1): either $(\theta_x^{r+H(x)}, \sigma(\theta_x^{r+H(x)}))$ or $(\tilde{\theta}_x, \theta_y^{r+H(y)})$, with $\sigma(\tilde{\theta}_x) = \theta_y^{r+H(y)}$, that is

$$\tilde{\theta}_x = M_x + (\theta_x^r - M_x)\left(\frac{\theta_y^{r+H(y)} - M_y}{\theta_y^r - M_y}\right)^{\frac{\gamma_x}{\gamma_y}}.$$

The area corresponding to initial conditions below the separatrix curve can be calculated as follows.

Lemma 3.1: Let $M_x, M_y, \theta_x^i, \theta_y^i \geq 0$ and $\gamma_x, \gamma_y > 0$. Given a domain B^r from which transitions are possible to the domains B^x and B^y, consider the corresponding separatrix curve (5), with endpoint (θ_x^r, θ_y^r). Define, for $s \in \{x, y\}$,

$$s_{\text{ini}} = \min\{\theta_s^r, \theta_s^{r+H(s)}\}, \qquad s_{\text{end}} = \max\{\theta_s^r, \theta_s^{r+H(s)}\}$$

and

$$\alpha = \begin{cases} \theta_x^r, & \text{if } \theta_x^r < x,\ \forall x \in B^r \\ \max\{\theta_x^{r+H(x)}, \tilde{\theta}_x\}, & \text{if } \theta_x^r > x,\ \forall x \in B^r, \end{cases}$$

$$\beta = \begin{cases} \min\{\theta_x^{r+H(x)}, \tilde{\theta}_x\}, & \text{if } \theta_x^r < x,\ \forall x \in B^r \\ \theta_x^r, & \text{if } \theta_x^r > x,\ \forall x \in B^r. \end{cases}$$

The area of the box B^r under the curve (5) is given by:

$$A_\sigma = \int_\alpha^\beta \sigma(x)dx + \sigma(\alpha)(\alpha - x_{\text{ini}}) + \sigma(\beta)(x_{\text{end}} - \beta) - y_{\text{ini}}(x_{\text{end}} - x_{\text{ini}}).$$

where the integral $\int_\alpha^\beta \sigma(x)dx$ is given by

$$M_y(\beta - \alpha) + \frac{\gamma_x}{\gamma_x + \gamma_y}(\theta_y^r - M_y)(\theta_x^r - M_x) \times \left(\left(\frac{\beta - M_x}{\theta_x^r - M_x}\right)^{1+\frac{\gamma_y}{\gamma_x}} - \left(\frac{\alpha - M_x}{\theta_x^r - M_x}\right)^{1+\frac{\gamma_y}{\gamma_x}}\right).$$

Furthermore, the area A_σ reflects the basin of attraction of B^r from where transitions are possible to B^x (if $\theta_y^r > y$ forall $y \in B^r$) or B^y (if $\theta_y^r < y$ forall $y \in B^r$).
In any case, note that either $\alpha = x_{\text{ini}} = \theta_x^r$ or $\beta = x_{\text{end}} = \theta_x^r$, so the expressions for A_σ can be simplified. The last term represents the area of the box just below B^r (which is counted in the integration) (it is naturally zero if there is no box below B^r, i.e. $y_{\text{ini}} = 0$).

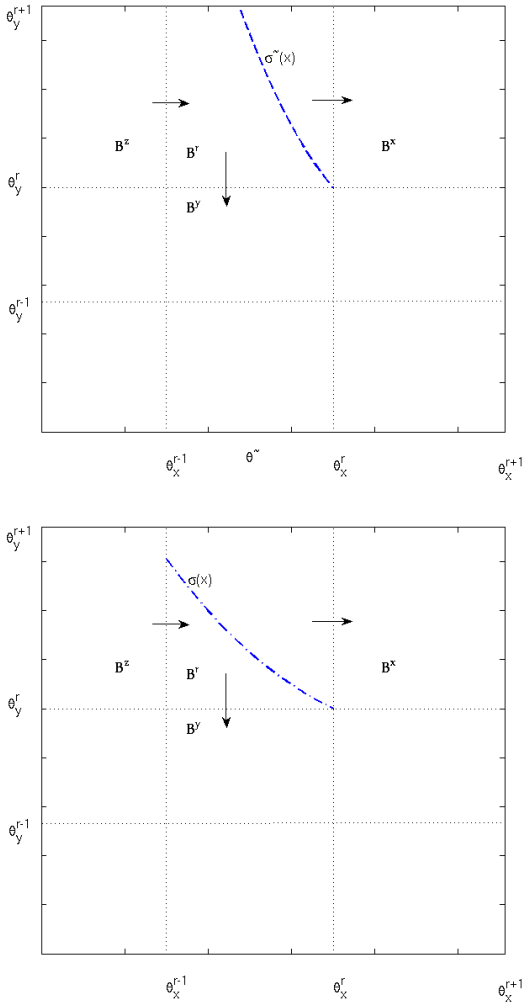

Fig. 1. A general case: inside the initial box B^r, there are two possibilities for the starting point of curve σ, depending on the parameters.

B. Probabilities of transition

To develop a definition of transition probability, consider the region B^z preceding B^r, meaning that coordinate z changes in the transition $B^z \to B^r$. Under assumption H1, observe that either coordinate z coincides with x or y (as in Fig. 1, where z coincides with x), or coordinate z is different from both x, y and thus introduces a third dimension on the transition scheme (in the Fig. 1, B^z would correspond to a cube above or below B^r, along a third direction z).

If B^z and B^r differ on coordinate x, then the boundary between B^z and B^r is a plane along $x_{z|r} = \theta_x^{r+H(x)}$. The probability of a transition $B^z \to B^r \to B^x$ is thus proportional to the *segment* of the boundary between B^z and B^r that lies below the separatrix $\sigma(x_{z|r})$, that is the intersection of the boundary and the separatrix.

If B^z introduces a new coordinate z, then the separatrix $\sigma(x)$ extends into a surface along the z direction. The transition from B^r to B^x or B^y depends on the point of this surface where the trajectory crosses from B^z to B^r. In

this case, the probability of a transition $B^z \to B^r \to B^x$ is still proportional to the *area* of the boundary between B^z and B^r that lies below $\sigma(x_{z|r})$, that is the intersection of the boundary and the separatrix.

Recall the notation $B^r = B^{k_1 \cdots k_n}$, and $B^x = B^{k_1 \cdots \tilde{k}_x \cdots k_n}$, where $\tilde{k}_x \in \{k_x - 1, k_x + 1\}$.

Definition 3.2: Consider a trajectory $\varphi(t; x_0)$ that crosses from a domain B^z to B^r, and assume that there are two possible transitions from B^r, to B^x or B^y. The *probability of transition between B^r and B^x, given B^z* is defined as:

$$P_{rx}(z) = \begin{cases} \frac{A_\sigma}{\left|\theta_x^r - \theta_x^{r+H(x)}\right| \left|\theta_y^r - \theta_y^{r+H(y)}\right|}, \\ \qquad \text{if } z \notin \{x, y\} \text{ or } B^z = B^r \\ \frac{|\theta_x^r - \beta|}{\left|\theta_x^r - \theta_x^{r+H(x)}\right|}, \qquad \text{if } z = x \end{cases} \tag{6}$$

where β is as defined in Lemma 3.1 and, in the case $z = x$, x is the coordinate such that $\hat{k}_x = k_x \neq \tilde{k}_x$, while $\hat{k}_y = k_y = \tilde{k}_y$. In addition, for each fixed z: $P_{rx}(z) + P_{ry}(z) = 1$.

IV. EXAMPLE: OSCILLATIONS IN BIOLOGICAL REGULATORY NETWORKS

To illustrate the applications of the concept of transition probability, we will consider a 3-dimensional system, consisting of two intertwinned negative feedback loops (Fig. 2). It is inspired by a reduced model of the NF-κB /IκB system

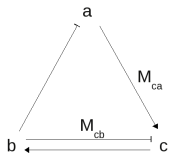

Fig. 2. Network consisting of two negative loops.

(see [10] for more details), where a =[NF-κB]$_{cytoplasm}$, b =[IκB], and c =[NF-κB]$_{nucleus}$. Oscillatory behaviour has been experimentally observed for this system [9]. A positive activation $x \to y$ will be described by a Heaviside function:

$$s^+(x, \theta_{xy}) = \begin{cases} 0, & x < \theta_{xy} \\ 1, & x > \theta_{xy} \end{cases}$$

and an inhibition $x \dashv y$ will be described similarly by $s^-(x, \theta_{xy}) = 1 - s^+(x, \theta_{xy})$. The model can be written in the piecewise constant framework as:

$$\begin{aligned} \dot{a} &= \gamma_a(s^-(b, \theta_{ba}) - a) \\ \dot{b} &= \gamma_b(s^+(c, 1) - b) \\ \dot{c} &= \gamma_c(M_{ca}s^+(a, \theta_a) + M_{cb}s^-(b, \theta_{bc}) - c), \end{aligned} \tag{7}$$

where we have assumed, to reduce the number of parameters, that the maximal values of a and b have been normalized to 1, and that $\theta_c = 1$. We will assume that the parameters satisfy the inequalities

$$\begin{aligned} &0 < \theta_a < 1, \quad 0 < \theta_{bc} < \theta_{ba} < 1, \\ &0 < M_{cb} < 1 < M_{ca}. \end{aligned} \tag{8}$$

Under these conditions, variable a has two regions (corresponding to one threshold quantity) and b, c both have three regions (two threshold quantities). So the state space can be divided into 18 regions, which can be labelled B^{ijk}, where $i \in \{0, 1\}$ and $j, k \in \{0, 1, 2\}$.

We have chosen parameters satisfying conditions (8) because they imply that system (7) has no stable steady states but its transition graph has several transition cycles. For reasons of space we omit the construction of the full transition diagram and show only the final result (see Fig. 3), where transient states are not included. Indeed, it can be easily shown that B^{002}, B^{110}, B^{111}, B^{120}, and B^{121} are transient domains, that is, once a trajectory leaves one of these domains, it will never return to it. Therefore, Fig. 3 represents the asymptotic behaviour of the system. The transition diagram has five distinct transition cycles in the sense of Definition 2.1: one cycle of length 6 ($c6$) and two cycles each of length 8 ($c8a$, $c8b$) and 10 ($c10a$, $c10b$). These are characterized in Definition 5.1. In particular, note that each of the domains represented in Fig. 3 has at most *two successors*, the only domains that admit two successors being B^{112}, B^{012}, and B^{021}. The method described in Section III can thus be applied, since hypotheses H1 is satisfied.

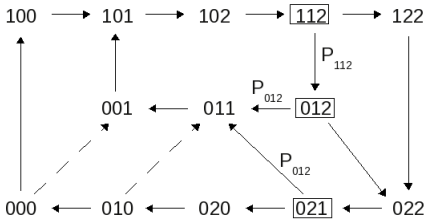

Fig. 3. Attractor for the discrete system Σ, representing the asymptotic behaviour of system (7).

The dynamics of system (7) under condition (8) is thus expected to exhibit oscillatory solutions following one of the five transition cycles. Among other results, given a set of parameters, we would like to predict which cycle is more likely to be followed by the solutions of the system.

A. Computing transition probabilities

The probabilities of transition associated with each arrow in the graph of Fig. 3 can be computed according to Definition 3.2. For the states where only one transition is possible the probability is, of course, equal to 1. Define the following new parameters, which represent the relative distances between thresholds:

$$B = \frac{1 - \theta_{ba}}{1 - \theta_{bc}}, \qquad C = \frac{M_{ca}}{1 - M_{cb}}. \tag{9}$$

Note that $B, C > 1$, by assumption on the parameters. Then the transition probabilities can be easily written in terms of B and C, and the ratios between degradation rates:

$$g_{ab} = \frac{\gamma_a}{\gamma_b}, \quad g_{bc} = \frac{\gamma_b}{\gamma_c}.$$

For simplicity of notation, we will abbreviate: $P_{112} \equiv P_{112 \to 012}$, $P_{012} \equiv P_{012 \to 011}$, and $P_{021} \equiv P_{021 \to 011}$.

Proposition 4.1: The probabilities of transition associated with the graph of Fig. 3 are given by:

$$P_{112} = \frac{\beta - 1}{\frac{1}{\theta_a} - 1}, \quad \beta = \min\left\{\frac{1}{\theta_a}, B^{g_{ab}}\right\};$$

$$P_{021} = \frac{\beta - 1}{\frac{1}{\theta_{bc}} - 1}, \quad \beta = \min\left\{\frac{1}{\theta_{bc}}, \frac{1}{M_{cb}^{g_{bc}}}\right\};$$

$$P_{012} = \begin{cases} 1 - \frac{1}{(C-1)(B-1)}\left[C(C^{g_{bc}} - 1) - \frac{C^{g_{bc}+1}-1}{1+\frac{1}{g_{bc}}}\right], \\ \qquad\qquad \text{if } B > C^{g_{bc}} \\ \frac{1}{C-1}\left[\frac{1}{1+\frac{1}{g_{bc}}}\frac{B^{1+\frac{1}{g_{bc}}}-1}{B-1} - 1\right], \quad \text{if } B < C^{g_{bc}}; \end{cases}$$

$$P_{010\to 000} = 1;$$

$$P_{000\to 100} = 1.$$

Proof: For the case $102 \to 112 \to 122, 012$: the rectangle 112 corresponds to $a \in (\theta_a, 1)$, $b \in (\theta_{ba}, \theta_{bc})$ and $c \in (\theta_c, M_{ca})$. The coordinate c is constant throughout these regions, and the coordinate b strictly decreases along $102 \to 112 \to 012$, so we will take $z = a$, $x = a$, and $y = b$, with $\theta_x^r = \theta_a$, $H(x) = 1$ and $\theta_y^r = \theta_{bc}$, $H(y) = -1$. The result follows from (6), with $z = x$. The values of the constants can be obtained by looking at the equations in box B^{112}: $M_x = 0$, $M_y = 1$, $\theta_x^{r+H(x)} = 1$, $\theta_y^{r+H(y)} = \theta_{ba}$.

For the case $112 \to 012 \to 022, 011$: the rectangle 012 corresponds to $a \in (0, \theta_a)$, $b \in (\theta_{ba}, \theta_{bc})$ and $c \in (\theta_c, M_{ca} + M_{cb})$. In the two transitions from 012 the coordinate a remains constant, so we will take $z = a$, $x = b$, and $y = c$, with $\theta_x^r = \theta_{bc}$, $H(x) = -1$ and $\theta_y^r = \theta_c$, $H(y) = 1$. So the result follows from (6), with $z \notin \{x, y\}$. To find the constants, observe that the equations in box B^{012} are: $\dot{b} = k_b - \gamma_b b$ and $\dot{c} = k_{cb} - \gamma_c c$. Therefore, $M_x = 1$ and $M_y = M_{cb}$, and $\theta_x^{r+H(x)} = \theta_{ba}$, $\theta_y^{r+H(y)} = M_{ca} + M_{cb}$.

The other cases can be similarly analysed. ∎

From Proposition 4.1 it follows that there is, in fact, only one possible transition from 010 and from 000. The transition graph can thus be simplified, by removing the dashed arrows in 3.

B. Parameter identifiability and estimation

In the present framework, the working hypothesis is that the transition probabilities are an output of the system, that is, they can be experimentally measured. In this example, there are only three independent probabilities: P_{112}, P_{012}, and P_{021}, so one may expect to be able to estimate at most three quantities/functions on the parameters of the system, including some of the thresholds. The independent parameters of the system are: θ_a, θ_{ba}, θ_{bc}, M_{ca}, M_{cb}, g_{ab}, and g_{bc}. From Proposition 4.1, the parameters that satisfy any given triple of probabilities can be fully characterized:

Proposition 4.2: Consider a triple of probabilities $P_{112} \in (0, 1]$, $P_{021}, P_{012} \in (0, 1)$. The family of parameters that satisfy Proposition 4.1 are given by $B, C > 1$, as given by (9), and either

$$F_1(B) > \max\left\{B^{\frac{1}{g_{bc}}} - 1, \frac{1}{\left(\frac{P_{021}}{B-1} + 1\right)^{\frac{1}{g_{bc}}} - 1}\right\} \tag{10}$$

with

$$C - 1 = F_1(B) = \frac{1}{P_{012}}\left[\frac{1}{1+\frac{1}{g_{bc}}}\frac{B^{1+\frac{1}{g_{bc}}}-1}{B-1} - 1\right]$$

or

$$C^{g_{bc}} - 1 \le F_2(C) < \frac{P_{021}}{\left(\frac{C}{C-1}\right)^{g_{bc}} - 1} \tag{11}$$

with

$$B - 1 = F_2(C) = \frac{1}{1 - P_{012}}\frac{1}{C-1}\left[C(C^{g_{bc}} - 1) - \frac{C^{g_{bc}+1} - 1}{1 + \frac{1}{g_{bc}}}\right]$$

For both cases (10) and (11), the other parameters are given by:

$$\left(\frac{B-1}{P_{021} + B - 1}\right)^{\frac{1}{g_{bc}}} < M_{cb} < \frac{C-1}{C}, \tag{12}$$

and

$$M_{ca} = C(1 - M_{cb}),$$

$$\theta_a \begin{cases} = \frac{P_{112}}{P_{112}+B^{g_{ab}}-1}, & P_{112} < 1 \\ > 1/B^{g_{ab}}, & P_{112} = 1 \end{cases} \tag{13}$$

$$\theta_{bc} \begin{cases} = \frac{P_{021}}{P_{021}+1/M_{cb}^{g_{bc}}-1}, & P_{021} < 1 \\ > M_{cb}^{g_{bc}}, & P_{021} = 1 \end{cases} \tag{14}$$

$$\theta_{ba} = 1 - B(1 - \theta_{bc}). \tag{15}$$

Thus, by measuring probabilities of transition, one may recover an interval for the ratio B (or C) between the magnitudes of the thresholds for the variable b. Then the ratio C follows from the value of B. The values B and C define an interval for the parameter M_{cb}. The threshold θ_a can be calculated directly from P_{112} and B; the thresholds θ_{ba} and θ_{bc} can be calculated from P_{021}, B, and M_{bc}.

To visualize these conditions, we will consider in more detail the case of equal degradation rates: $g_{ab} = g_{bc} = 1$. In this case, the interval defined by (11) is nonempty. The sets of possible parameters are depicted in Fig. 4.

Corollary 4.3: Assume $g_{ab} = g_{bc} = 1$ and consider a triple of probabilities $P_{021}, P_{112} \in (0, 1]$, $P_{012} \in (0, 1)$. If $P_{021} = 1$, then the parameters satisfy

$$B > C > 1, \quad M_{cb} < \frac{B-1}{2P_{012} + B - 1}, \quad \theta_{bc} > M_{cb}.$$

If $P_{021} < 1$, then there is an nonemtpy set of parameters only if $P_{021} > 2P_{012}$ and

$$B > \frac{1}{1 - P_{021}}, \text{ with } C = 1 + \frac{B-1}{2P_{012}}$$

and

$$\frac{B-1}{P_{021} + B - 1} < M_{cb} < \frac{B-1}{2P_{012} + B - 1}.$$

In both cases, $M_{ca} = C(1 - M_{cb})$ and θ_a, θ_{bc}, θ_{ba} are given by (13)-(15).

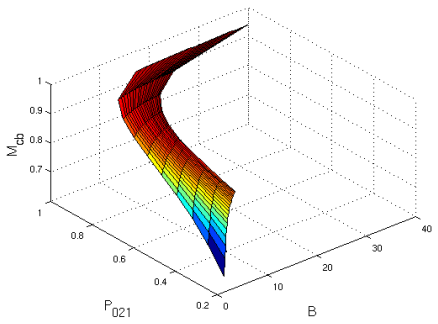

Fig. 4. Range of values admitted for B and M_{cb} in terms of P_{021}, in the case of equal degradation constants. The case $P_{012} = 0.1$ is shown.

V. CONTROLLING THE SYSTEM

The attractor on Fig. 3 has 5 different transition cycles, as indicated at the beginning of Section IV. In this context, Propositions 4.1 and 4.2 can be used as a guide for choosing parameters that yield a system with a periodic orbit of a given length, or passing through desired domains. For instance, it is clear that setting $P_{021} = 1$ prevents a cycle of length 10. Similarly, setting $P_{112} = 1$ and choosing a large P_{012} leads to a high probability of obtainning a length 6 cycle. Another application of the previous results is to control system (7) between two cycles, by changing only a small set of parameters.

A. Predicting the transition cycle

To formalize the idea that the orbit of system (7) follows a given transition cycle with a certain probability, we will now assume that the system has a unique stable periodic orbit and, for each set of parameters, define a *predicted transition cycle*.

Definition 5.1: Given any set of parameters, the probability that a periodic orbit of system (7) follows one of the transition cycles is:

$$\begin{aligned} P(c6) &= P_{112}P_{012}, \\ P(c8a) &= P_{112}(1-P_{012})P_{021}, \\ P(c8b) &= (1-P_{112})P_{021}, \\ P(c10a) &= P_{112}(1-P_{012})(1-P_{021}), \\ P(c10b) &= (1-P_{112})(1-P_{021}). \end{aligned}$$

The *predicted transition cycle* to be followed by the periodic orbit is $\tilde{c}$ such that:

$$P(\tilde{c}) = \max\{P(c6), P(c8a), P(c8b), P(c10a), P(c10b)\}.$$

Note that the five probabilities add up to 1. Since the computation of transition probabilities are based on a model, an immediate question is whether the predicted transition cycle is a reasonable indication of the actual observed cycle. Performing simulations by randomly choosing sets of parameters, shows that the predicted transition cycle is correct on around 75% of the simulations (see also Fig. 5). Note that, if $P_{112} = P_{021} = 1$, only the transition cycles $c6$ or $c8a$ may take place. In this case, $P(c6) + P(c8a) = 1$ so, if the prediction fails, the predicted probability is simply $1 - P$(observed cycle) (this accounts for the distribution of the red crosses in Fig. 5).

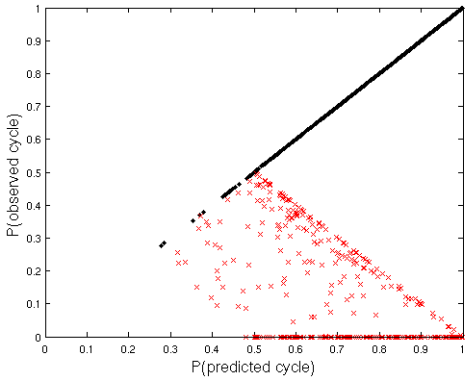

Fig. 5. Probability of the actually observed cycle againtst that of the predicted transition cycle. Results from 1000 simulations: black dots represent cases where the predicted cycle coincides with the observed cycle; red crosses represent the cases where prediction fails.

These simulations also show that length 8 transition cycles are the most frequent (Fig. 6). The largest discrepancy between the number of predicted and observed cycles concerns length 6 and 10 cycles: overall, the transition probability model predicts 4% more $c6$ cycles and 4% less $c10$ cycles than are observed.

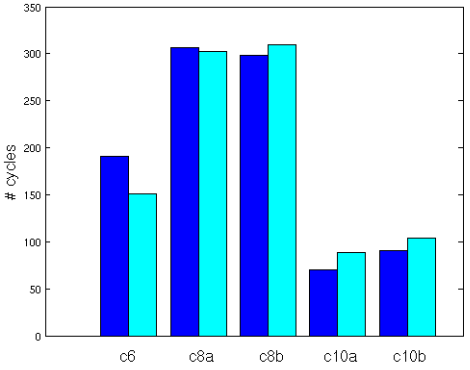

Fig. 6. Histograms of the distribution of transition cycles over 1000 simulations. Dark blue bars represent predicted cycles and light blue bars represent observed cycles.

B. Controlling the system to a given cycle

Finally, we will use Definition 5.1 in conjunction with Propositions 4.1 and 4.2 to construct a control that drives the system to follow a desired cycle. Throughout this section, it will be assumed that the production rates M_{ca} and M_{cb} can be controlled. These can be associated to the "weights" of each of the negative feedback loops in the dynamics of the system: note that the system with $M_{cb} = 0$ is a single 3-dimensional negative feedback loop. This system has a unique stable periodic orbit, following cycle $c6$, as shown in [4].

Thus, in Propositions 5.2 to 5.4 below it will be assumed that θ_a, θ_{ba}, and θ_{bc} are given, and that $g_{ab} = g_{bc} = 1$, for simplicity. Under this assumption, the parameter B and the probability P_{112} are also given.

Proposition 5.2: The predicted transition cycle is of length 10 if

$$M_{cb} > \frac{2\theta_{bc}}{1+\theta_{bc}},$$
$$M_{ca} > (1-M_{cb})\left(1+\frac{B-1}{2}\frac{G(M_{cb})}{\frac{1}{\theta_{bc}}-\frac{1}{M_{cb}}}\right)$$

where

$$G(M_{cb}) = \max\left\{\frac{2}{\theta_{bc}}-\frac{1}{M_{cb}}-1,\ \frac{P_{112}}{1-P_{112}}\left(\frac{1}{\theta_{bc}}-1\right)\right\},$$

if $P_{112} < 1$ and

$$G(M_{cb}) = \frac{2}{\theta_{bc}}-\frac{1}{M_{cb}}-1, \text{ if } P_{112}=1.$$

if

The proof follows from Corollary 4.3 by requiring that $P(c10i) > P(c8i)$ and $P(c10i) > P(c6)$ $(i = a, b)$.

Proposition 5.3: Assume $P_{112} < 1$. The predicted transition cycle is of length 8 if

$$\theta_{bc} < M_{cb} < \frac{2\theta_{bc}}{1+\theta_{bc}},$$
$$M_{ca} > (1-M_{cb})\left(1+\frac{B-1}{2}\frac{P_{112}}{1-P_{112}}\frac{\frac{1}{\theta_{bc}}-1}{\frac{1}{M_{cb}}-1}\right)$$

or

$$M_{cb} < \theta_{bc},$$
$$M_{ca} > (1-M_{cb})\left(1+\frac{B-1}{2}\max\left\{\frac{1}{2},\frac{P_{112}}{1-P_{112}}\right\}\right).$$

If $P_{112} = 1$, then the predicted transition cycle is of length 8 if

$$\theta_{bc} < M_{cb} < \frac{2\theta_{bc}}{1+\theta_{bc}}, \quad M_{ca} > 1$$

or

$$M_{cb} < \theta_{bc}, \quad M_{ca} > (1-M_{cb})\left(1+\frac{1}{2}\frac{B-1}{2}\right).$$

The proof is similar to that of Proposition 5.2.

Proposition 5.4: Assume $P_{112} \leq 1$. The predicted transition cycle is of length 6 if

$$M_{cb} < \theta_{bc},$$
$$M_{ca} < (1-M_{cb})\left(1+\frac{B-1}{2}\min\left\{\frac{1}{2},\frac{P_{112}}{1-P_{112}}\right\}\right).$$

The proof is again similar to the previous ones, using the fact that the inequality $P(c6) > P(c8a)$ can only be satisfied if $P_{021} = 1$.

As an numerical example, one of the randomly generated sets of parameters was:

$$\theta_a = 0.7513, \quad \theta_{ba} = 0.2551, \quad \theta_{bc} = 0.6320,$$
$$M_{cb} = 0.6991, \quad M_{ca} = 3.6727. \tag{16}$$

TABLE I

PROBABILITIES OF TRANSITION

	Original set	Prop. 5.4	Prop. 5.2
M_{cb}	0.6991	0.1937	0.9324
M_{ca}	3.6727	1.0064	3.6727
P_{112}	1.0	1.0	1.0
P_{021}	0.7392	1.0	0.1246
P_{012}	0.0457	0.8789	0.0096
$P(c6)$	0.0457	0.8789	0.0096
$P(c8a)$	0.7054	0.1211	0.1234
$P(c8b)$	0.0	0.0	0.0
$P(c10a)$	0.2489	0.0	0.8670
$P(c10b)$	0.0	0.0	0.0

The corresponding transition probabilities and each cycle probabilities are shown in Table I (Original set column). The predicted transition cycle is $c8a$, which indeed corresponds to the observed periodic orbit (see Fig. 7).

To control the system towards a length 6 cycle, we have used Proposition 5.4. Since $P_{112} = 1$, and to guarantee that $M_{ca} > 1$, we choose $M_{cb} < \min\{\theta_{bc}, 0.95(1-1/(1+(B-1)/4)\}$, and next set $M_{ca} = 0.5 + 0.5 * (1-M_{cb})(1+(B-1)/4)$. To control the system towards a length 10 cycle, we have used Proposition 5.4, choosing $M_{cb} = 0.7 + 0.3 \times 2\theta_{bc}/(1+\theta_{bc})$ This consists of increasing the contribution from the short negative feedback loop. Computing the new lower bound for M_{ca} shows that the same value for M_{ca} can be used. The new parameters and transition probabilities are given in Table I. For both cases, the predicted transition cycle is correct, as can be seen in Figs. 8 and 9.

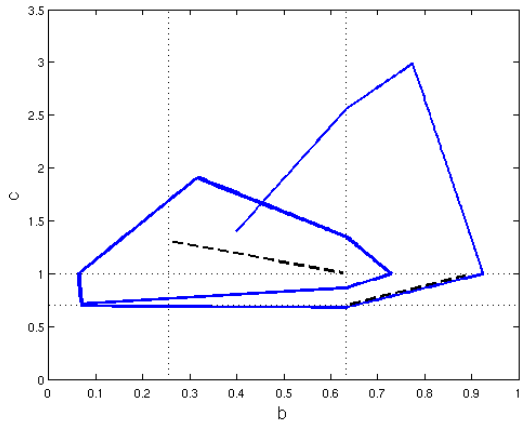

Fig. 7. The projection on the plane bc of the periodic orbit of system (7) with parameters (16), which follows a cycle of length 8. The dashed lines represent the separatrices σ in domains B^{112} and B^{021}.

VI. CONCLUSIONS AND FUTURE WORK

A notion of transition probability has been introduced to relate the parameters of piecewise affine systems with the qualitative dynamics in the corresponding transition graph. The transition probability depends on the volume of initial conditions that cross from the current domain to a neighbouring domain, and also on the previous step history of the

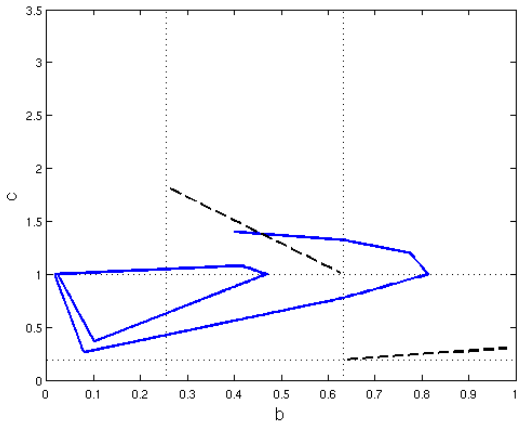

Fig. 8. Controlling the system to a periodic orbit that follows a length 6 transition cycle. The projection on the plane bc of the periodic orbit of system (7) with parameters (16), except $M_{cb} = 0.1937$ and $M_{ca} = 1.0064$.

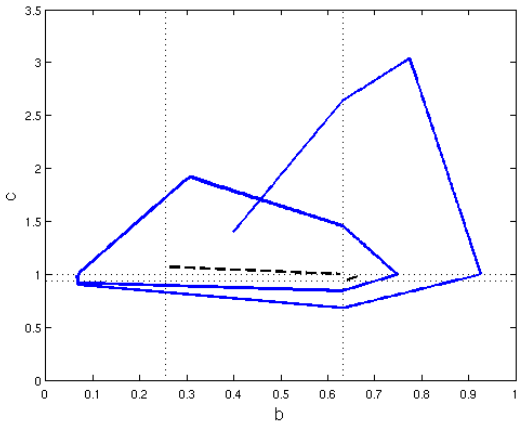

Fig. 9. Controlling the system to a periodic orbit that follows a length 10 transition cycle. The projection on the plane bc of the periodic orbit of system (7) with parameters (16), except $M_{cb} = 0.9324$.

trajectory. Therefore, this notion of transition probability can be interpreted as a very rough approximation of a first return map. Applications of this idea include parameter estimation, system control by finding sets of parameters that satisfy a certain qualitative dynamics, and, in the case of systems with several possible transition cycles, the prediction of the most likely periodic orbit of the system given a set of parameters.

This study deals only with systems where there are at most two possible transitions from each hyperrectangle, which is a very limiting constraint. The generalization of probabilities for multiple transitions and application to higher dimensional systems constitute directions for future work.

REFERENCES

[1] R. Casey, H. de Jong, and J.L. Gouzé. Piecewise-linear models of genetic regulatory networks: equilibria and their stability. *J. Math. Biol.*, 52:27–56, 2006.

[2] R. Edwards. Analysis of continuous-time switching networks. *Physica D*, 146:165–199, 2000.

[3] E. Farcot and J.L. Gouzé. A mathematical framework for the control of piecewise-affine models of gene networks. *Automatica*, 44(9):2326–2332, 2008.

[4] E. Farcot and J.L. Gouzé. Periodic solutions of piecewise affine gene network models with non uniform decay rates: the case of a negative feedback loop. *Acta Biotheor.*, 57:429–455, 2009.

[5] L. Glass and S.A. Kauffman. The logical analysis of continuous, nonlinear biochemical control networks. *J. Theor. Biol.*, 39:103–129, 1973.

[6] L. Glass and J.S. Pasternak. Stable oscillations in mathematical models of biological control systems. *J. Math. Biol.*, 6:207–223, 1978.

[7] J.L. Gouzé and M. Chaves. Piecewise affine models of regulatory genetic networks: review and probabilistic interpretation. In J. Lévine and P. Müllhaupt, editors, *Advances in the Theory of Control, Signals and Systems, with Physical Modelling*, Lecture Notes in Control and Information Sciences. Springer, 2010. to appear.

[8] J.L. Gouzé and T. Sari. A class of piecewise linear differential equations arising in biological models. *Dyn. Syst.*, 17(4):299–316, 2002.

[9] A. Hoffmann, A. Levchenko, M.L. Scott, and D. Baltimore. The IkB-NFkB signaling module: temporal control and selective gene activation. *Science*, 298:1241–1245, 2002.

[10] L. Tournier and M. Chaves. Uncovering operational interactions in genetic networks using asynchronous boolean dynamics. *J. Theor. Biol.*, 260(2):196–209, 2009.